Identification of transcription factors regulating senescence in wheat through gene regulatory network modelling

Borrill, Philippa; Harrington, Sophie A; Simmonds, James; Uauy, Cristobal

DOI:
10.1104/pp.19.00380

Document Version
Peer reviewed version

Citation for published version (Harvard):
Borrill, P, Harrington, SA, Simmonds, J & Uauy, C 2019, 'Identification of transcription factors regulating senescence in wheat through gene regulatory network modelling', *Plant Physiology*, vol. 180, no. 3, pp. 1740-1755. https://doi.org/10.1104/pp.19.00380

Short title: Transcription factors regulating wheat senescence

Author for contact: Philippa Borrill (p.borrill@bham.ac.uk), School of Biosciences, University of Birmingham, Birmingham, B15 2TT, UK and Cristobal Uauy (cristobal.uauy@jic.ac.uk), John Innes Centre, Norwich Research Park, NR4 7UH, UK

Article title:

Identification of transcription factors regulating senescence in wheat through gene regulatory network modelling

Authors: Philippa Borrill[1]†, Sophie A. Harrington[2], James Simmonds[2], Cristobal Uauy[2]†

[1] School of Biosciences, University of Birmingham, Birmingham, B15 2TT, UK.

[2] Department of Crop Genetics, John Innes Centre, Norwich Research Park, NR4 7UH, UK.

† Corresponding authors: Philippa Borrill (p.borrill@bham.ac.uk) and Cristobal Uauy (cristobal.uauy@jic.ac.uk)

One sentence summary: Integrating gene regulatory network modelling during a gene expression timecourse with publicly available genomic datasets identifies transcription factors regulating senescence in wheat.

Footnotes:

Author contributions

PB and CU conceived, designed and coordinated the study. PB harvested tissue for the timecourse and collected the associated chlorophyll and grain moisture content phenotypic data. PB carried out the RNA extraction, analysed the RNA-Seq data, and built the gene regulatory network model. PB identified mutations in *NAM-A2* and *NAM-B2* for crossing and designed KASP markers. JS carried out crossing of *NAM-A2* and *NAM-B2* mutant lines. JS and PB carried out KASP genotyping. PB and SH carried out phenotyping of the *NAM2* mutant lines. PB wrote the manuscript. CU, SH, and JS edited the manuscript.

Funding information

This work was supported by the UK Biotechnology and Biological Sciences Research Council (BBSRC) through an Anniversary Future Leader Fellowship to P.B. (BB/M014045/1) and the Designing Future Wheat (BB/P016855/1) and GEN (BB/P013511/1) ISPs. S.A.H. was supported by the John Innes Foundation. This research was also supported in part by the NBI Computing infrastructure for Science (CiS) group through the HPC resources.

Email address of author for contact: p.borrill@bham.ac.uk and cristobal.uauy@jic.ac.uk

Abstract

Senescence is a tightly regulated developmental programme coordinated by transcription factors. Identifying these transcription factors in crops will provide opportunities to tailor the senescence process to different environmental conditions and regulate the balance between yield and grain nutrient content. Here, we use ten time points of gene expression data along with gene network modelling to identify transcription factors regulating senescence in polyploid wheat (*Triticum aestivum* L.). We observe two main phases of transcriptional changes during senescence: early downregulation of housekeeping functions and metabolic processes followed by upregulation of transport and hormone related genes. These two phases are largely conserved with Arabidopsis (*Arabidopsis thaliana*), although the individual genes underlying these changes are often not orthologous. We have identified transcription factor families associated with these early and later waves of differential expression. Using gene regulatory network modelling, we identified candidate transcription factors that may control senescence. Using independent, publicly available datasets, we found that the most highly ranked candidate genes in the network were enriched for senescence-related functions compared to all genes in the network. We validated the function of one of these candidate transcription factors in senescence using wheat chemically-induced mutants. This study lays the groundwork to understand the transcription factors that regulate senescence in polyploid wheat and exemplifies the integration of time-series data with publicly available expression atlases and networks to identify candidate regulatory genes.

Introduction

Grain yield and nutrient content in cereal crops is determined by the accumulation of carbon, nitrogen, and other nutrients in the grain towards the end of a plant's life. The availability of these nutrients is strongly influenced by the process of senescence, a regulated developmental programme to remobilise nutrients from the vegetative tissues to the developing grain. Both the onset and rate of senescence influence grain yield and nutrient content. A delay in senescence may be associated with increased yield due to an extended period of photosynthesis (Thomas and Howarth, 2000; Gregersen et al., 2013), although this is not always the case (Borrill et al., 2015a). Delayed senescence may also be associated with a decrease in grain nutrient content due to reduced nutrient remobilisation from green tissues (Distelfeld et al., 2014). Senescence is often associated with the visual loss of chlorophyll, however the initiation of senescence through signalling cascades, and early stages such as degradation of protein and RNA, are not visible (Buchanan-Wollaston et al., 2003; Fischer, 2012). Through these initial stages, and later during visual senescence, a programme of tightly-regulated changes occurs in gene expression (Buchanan-Wollaston et al., 2003; Fischer, 2012). Despite its importance, we know

relatively little about the molecular control of senescence in crops such as wheat (Distelfeld et al., 2014).

This lack of knowledge is partly due to the difficulty of identifying genes regulating quantitative traits in the large wheat genome (IWGSC et al., 2018) as well as the subtle effects of individual gene copies (homoeologs) within the polyploid context (Borrill et al., 2015b). These challenges mean that conventional genetic mapping approaches often take many years to identify causal genes. To date two genes have been identified to regulate senescence in wheat. The *NAM-B1* NAC transcription factor was identified to underlie a quantitative trait locus (QTL) for grain protein content and senescence (Uauy et al., 2006). A second NAC transcription factor, *NAC-S*, was found to have a strong correlation between its expression level and leaf nitrogen concentration in tandem with a role in regulating senescence (Zhao et al., 2015). However, to realise the potential to manipulate the rate and onset of senescence in wheat it will be necessary to gain a more comprehensive understanding of the network of transcription factors regulating this process. Identifying these transcription factors may enable the development of wheat varieties with a senescence profile tailored to maximise nutrient remobilisation whilst maintaining yield and providing adaption to local growing conditions.

The first step towards manipulating senescence at the molecular level is to understand the genes which are involved in the process, and the transcription factors which orchestrate gene expression changes during senescence. Over 50% of micro- and macro-nutrients remobilised to the developing grain originate from the uppermost (flag) leaf of the senescing wheat plant (Garnett and Graham, 2005; Kichey et al., 2007), making it a key tissue in which to understand the senescence process. Previous attempts have been made to characterise transcriptional changes in wheat flag leaves, however these studies have been either carried out with microarrays which were limited to a small set of 9,000 genes (Gregersen and Holm, 2007) or had a limited number of samples and time points (Pearce et al., 2014; Zhang et al., 2018). Decreases in the cost of RNA-Seq now mean that these constraints can be overcome through genome-wide expression studies across multiple time points. The recent publication of the wheat genome sequence with over 100,000 high confidence gene models (IWGSC et al., 2018) and accompanying functional annotations, enhances the ease and accuracy with which RNA-Seq data can be analysed in wheat. Systems biology approaches can start to make sense of the vast quantities of data produced and identify the regulatory pathways controlling quantitative traits (Kumar et al., 2015).

Our aim in this study was to identify the molecular pathways involved in senescence in wheat and to determine candidate transcription factors controlling these processes in the flag leaf. We sequenced a ten time point expression timecourse of wheat senescence in the flag leaf from 3 days post anthesis

104 until 26 days post anthesis which corresponded to the first signs of visual senescence. We identified
105 the temporal progression of the senescence process at the molecular level and used gene regulatory
106 network modelling to predict transcription factors which coordinate this developmental process. We
107 confirmed the role of one of these candidate genes, *TraesCS2A02G201800* (*NAM-A2*), in wheat itself.

Results

Growth and physiological measurements

To understand the transcriptional control of the initiation of senescence we harvested an early timecourse of senescence at 3, 7, 10, 13, 15, 17, 19, 21, 23, and 26 days after anthesis (DAA) (Fig. 1A). SPAD chlorophyll meter readings in the flag leaf were maintained at a similar level from 3 to 21 DAA, with a significant decrease from 23 DAA (Supplemental Fig. S1). Percentage moisture of the grains decreased from 80.0% at 3 DAA to 54.7% at 26 DAA which corresponds to the soft dough stage (GS85 (Zadoks et al., 1974)) (Supplemental Fig. S2), indicating that the time period sampled included the majority of the grain filling period.

Strong transcriptional changes occur during flag leaf senescence

RNA was extracted from the flag leaf blade with three replicates for each of the ten time points and sequenced. The RNA-Seq data was aligned to the RefSeqv1.1 transcriptome annotation (IWGSC et al., 2018) using kallisto (Bray et al., 2016). On average, each sample had 38.7 M reads, of which 30.9 M mapped (78.9%) (Supplemental Table S1). We found that 52,905 high confidence genes were expressed at > 0.5 transcripts per million (TPM) in at least one time point during flag leaf senescence, which corresponds to 49.0% of high confidence genes. To identify genes differentially expressed during the timecourse, we used two programmes specifically designed for timecourse data: ImpulseDE2 (Fischer et al., 2018) and gradient tool (Breeze et al., 2011). In total 9,533 genes were identified as differentially expressed by both programmes, giving a high confidence set of differentially expressed genes (DEGs). In addition, gradient tool identified the time points at which the genes became differentially expressed which we used to determine the temporal changes in gene expression associated with senescence (Supplemental Table S2).

To define the biological roles of these 9,533 genes, we grouped them according to the first time point at which they were up or downregulated. For example, a gene first upregulated at 10 DAA was in group “U10” (up 10 DAA), whereas a gene first downregulated at this time point was assigned to group “D10” (down 10 DAA). Fewer than 4% of genes were both up and down regulated during the timecourse and these were excluded from further analysis of global expression patterns, resulting in 17 expression patterns (Supplemental Table S2). In total, approximately twice as many genes were upregulated during this senescence timecourse than downregulated (5,343 compared to 2,715). This indicates that senescence is actively regulated through transcriptional upregulation rather than a general downregulation of biological processes.

We found that the patterns of up and downregulation were not equally spaced throughout the timecourse. During the early stages of senescence, the majority of DEGs were downregulated (825/1035 DEGs at 3 DAA), and these continued to be downregulated throughout the timecourse (Fig. 1B). At the later stages of senescence relatively few genes started to be downregulated (e.g. 50 genes at 19 DAA). Instead the number of genes which started to be upregulated increased from 210 genes at 3 DAA to 1,324 genes at 13 DAA. After this peak of upregulation at 13 DAA, fewer genes started to be upregulated, although there were still over 500 genes upregulated at each of 15, 17, and 19 DAA. Genes that were upregulated even at early stages of senescence tended to continue to increase in expression throughout the timecourse. At the latest stages of the timecourse, when chlorophyll loss was visible (23 and 26 DAA), very few genes started to be differentially expressed; no genes started to be downregulated at either time point or upregulated at 26 DAA, whilst only 31 genes started to be upregulated at 23 DAA (too few to be visible in Fig. 1B). The major shift from downregulation at the early stages of senescence to upregulation at the later stages was also observed in Arabidopsis (Breeze et al., 2011), and strikingly this occurs at a very similar period during the senescence process in both species, prior to the visual loss of chlorophyll (29 to 33 DAS in Arabidopsis and 13 to 21 DAA in wheat, Supplemental Fig S3).

We found that this temporal divide between downregulation at the early stages of senescence and upregulation at the later stages was also reflected in different GO term enrichments in these groups of DEGs (Fig. 1C; Supplemental Table S3). The large numbers of genes which started to be downregulated at 3 and 7 DAA were enriched for GO terms relating to housekeeping functions (e.g. translation, photosynthesis, and rRNA processing) as well as for central metabolic processes such as amino acid biosynthesis and starch biosynthesis. These are very similar to the results found in Arabidopsis where during senescence downregulated genes were significantly enriched for functions in photosynthesis and carbohydrate and amino acid metabolism (Breeze et al., 2011). Alongside these housekeeping functions, downregulated genes were enriched for defence responses and hormone biosynthesis and signalling, indicating a reduction in the transcriptional responses to stimuli. This differs from results in Arabidopsis where these GO terms were not enriched in downregulated genes. Later in the timecourse, from 10 to 13 DAA, groups of genes started to be upregulated which were involved in vesicle mediated transport and the proteasome, indicating a remobilisation of components from the existing proteins. This is supported by the upregulation from 13 DAA of genes involved in phosphate and protein transport. GO terms related to transport function were also enriched amongst the upregulated genes in Arabidopsis, but this was principally before anthesis, a time point we did not test (Breeze et al., 2011). From 15 DAA to 21 DAA waves of genes enriched for responses to cytokinin, ABA and ethylene were upregulated, indicating a temporal hierarchy of hormone responses during

senescence. This hierarchy appears to be conserved between wheat and Arabidopsis with both species showing earlier upregulation of genes enriched for ABA and JA signalling and responses (17 days after anthesis in wheat, 23 days after sowing in Arabidopsis) and later upregulation of genes enriched for ethylene signalling and responses (21 days and 33 days, respectively). However, the time separating these different hormone responsive genes is longer in Arabidopsis (Supplemental Fig. S3).

Conservation of senescence-related genes between wheat, rice and Arabidopsis

Given the high degree of conservation of enriched GO terms between up and downregulated genes in wheat and Arabidopsis, we compared the expression profiles of previously identified senescence-associated genes from Arabidopsis with their orthologs in wheat. We first explored ten genes from Arabidopsis which have been proposed as a basic set of genes to assess the progress of senescence (Bresson et al., 2017). We found that their expression profiles between Bresson et al. (2017) and Breeze et al. (2011) were largely consistent, although *CAT2* was described as a down-regulated gene in Bresson et al. (2017), whereas its expression was upregulated during senescence in Breeze et al. (2011) (Fig. 2, Supplemental Table S4), and *WRKY53* and *CAT3* were not differentially expressed in Breeze et al. (2011). We were able to identify wheat orthologs for seven of these ten genes, and four of these were differentially expressed during wheat senescence in a similar direction to that observed in Arabidopsis (Fig. 2). However, the wheat orthologs of two well-known senescence associated genes in Arabidopsis (*SAG12* and *ANAC092/ORE1*) were not differentially expressed during our wheat senescence timecourse, consistent with independent wheat RNA-Seq datasets (Fig. 2, Supplemental Table S4).

Since *ANAC092/ORE1*, part of a robust system controlling senescence in Arabidopsis (Kim et al., 2009), was not differentially expressed in wheat we investigated whether other NAC transcription factors (TFs) known to regulate senescence in Arabidopsis may be contributing to senescence in wheat instead. We focussed on nine additional NAC TFs that regulate senescence in Arabidopsis (Fig. 2, Supplemental Table S4). For five of these nine NACs, we were able to identify wheat orthologs. *AtNAP/ANAC029* was identified as a key regulator of senescence in Arabidopsis (Guo and Gan, 2006) and the ortholog in wheat displays a very similar increase in expression during senescence in our timecourse and in an independent dataset (Fig. 2, Supplemental Table S4), suggesting it too may play a role in regulating senescence in wheat. *ANAC082* and *ANAC090* form part of a NAC regulatory module that governs the shift from positive to negative regulation amongst NACs at a pre-senescence stage in Arabidopsis (Kim et al., 2018). However, *ANAC082* and *ANAC090* were not differentially expressed in Arabidopsis, and the majority of their wheat orthologs were also not differentially expressed during senescence (the third member of the regulatory module *ANAC017* did not have a wheat ortholog). In contrast two other NACs known to regulate senescence in Arabidopsis, namely

ANAC059/ORS1 (Balazadeh et al., 2011), a paralog of *ANAC092/ORE1*, and *ANAC042/JUB1* (Wu et al., 2012), were upregulated during the earlier part of the timecourse in Arabidopsis, but no change in expression was observed in the wheat orthologs. Together, these results show that although the broad scale biological processes governing senescence are similar between Arabidopsis and wheat, many of the individual genes influencing senescence are not conserved between the two species.

The lack of conservation between orthologous genes in wheat and Arabidopsis may be explained by their evolutionary separation ~200 million years ago when dicots and monocots diverged (Bowers et al., 2003; Wolfe et al., 1989). To put this finding in context, we examined the conservation of senescence-related genes in rice, a monocot species which is more closely related to wheat (50 million years since divergence (Charles et al., 2009)). Leng et al. (2017) identified 32 leaf senescence-related genes in rice, of which we identified 26 to have orthologs in wheat (Supplemental Table S5). We examined the expression of these rice genes during a timecourse of rice senescence from 4 to 28 days after heading (Lee et al., 2017). The majority of these genes with wheat orthologs (17 out of 26) had a conserved pattern of expression between wheat and rice (Supplemental Table S6). Five were upregulated in both species including *SGR* which regulates chlorophyll degradation in rice (Park et al., 2007), *OsNAC106* which inhibits leaf senescence (Sakuraba et al., 2015), and *OsNAP/PS1* which fine-tunes ABA biosynthesis and leaf senescence in rice (Liang et al., 2014). One gene (*LTS1/OsNaPRT1*) which plays a role in the NAD salvage pathway in rice (Wu et al., 2016) was downregulated in both species whilst eleven genes were not differentially expressed during leaf senescence in either species. Nine genes showed non-conserved patterns of expression between wheat and rice, including two genes affecting jasmonate content (*OsPME1* and *OsTSD2*) (Fang et al., 2016) that showed opposite expression patterns between rice (upregulated) and one wheat homoeolog (downregulated; the other homoeologs were not differentially expressed). Interestingly, of the seven senescence-related TFs examined from rice, four showed conserved expression patterns between rice and wheat. We were not able to identify wheat orthologs for the remaining three rice senescence-related TFs, suggesting that the transcriptional control of senescence is not completely conserved between wheat and rice, as previously demonstrated for *NAM-B1* (Distelfeld et al., 2012).

Transcription factors regulating senescence

We next examined TF expression patterns to understand how these highly ordered and coordinated transcriptional changes are regulated in wheat. We found that 2,210 TFs were expressed (> 0.5 TPM) during the timecourse but only 341 TFs (15.4%) were differentially expressed. A small number of TFs (18 TFs; 5.2%) were both up and downregulated during the timecourse (Supplemental Table S2), including *NAM-A1*, a known regulator of senescence in wheat. It is possible these TFs are bifunctional, acting to both activate and repress senescence-related pathways, similar to the positive and negative

241 regulation exerted by *ANAC083* on other senescence associated NACs in Arabidopsis (Kim et al., 2018).
242 We calculated the percentage of differentially expressed TF per TF family across time (Fig. 3). In
243 general, each TF family tended to either be upregulated or downregulated as a whole (Fig. 3), although
244 there are exceptions such as the C2C2_CO-like and MADS_II family which showed upregulation and
245 downregulation of different family members during the timecourse.

246 While we observed a temporal gradient of TF families starting to be up and downregulated throughout
247 the timecourse, we defined an initial (3 to 7 DAA) and later wave (13-19 DAA) when many TF families
248 were up or downregulated. TF families that were upregulated in the initial wave from 3 to 7 DAA
249 include the RWP-RK, pseudo ARR-B, and CCAAT_HAP2 (NF-YA) families (Fig. 3A). A distinct set of TF
250 families were upregulated in the later wave from 13 to 19 DAA including CAMTA, GRAS and MADS_II.
251 After these waves of upregulation were initiated, the same families tended to continue to be
252 upregulated throughout the rest of the timecourse. Compared to all genes, the RWP-RK, CCAAT_HAP2
253 (NF-YA), and NAC families were significantly enriched (padj <0.01, Fisher test; Fig. 3A) for upregulated
254 genes at early (RWP-RK and CCAAT_HAP2 (NF-YA)) and late (NAC) time points. In all three families,
255 over 30% of the expressed genes were upregulated during senescence corresponding to 61 NAC TFs
256 (32.4% of expressed NAC TFs) and eight RWP-RK and seven CCAAT_HAP2 (NF-YA) TFs (33.3% and
257 38.9% of expressed genes per family, respectively). The finding that NAC and CCAAT_HAP2 (NF-YA)
258 TFs are enriched for upregulated genes in senescing tissues is consistent with results in Arabidopsis
259 but, as discussed above, the exact gene family members involved in the senescence process may be
260 different between the two species. The RWP-RK family was not identified to be enriched for
261 upregulation in Arabidopsis, although this may be due to the RWP-RK genes being included within the
262 NLP family in the Arabidopsis analysis (Breeze et al., 2011).

263 In parallel with certain TF families being upregulated, another group of TF families were
264 downregulated during the senescence timecourse. The initial wave of downregulation largely
265 occurred at 7 DAA and included the AS2/LOB, bHLH_TCP, and MADS_I families. The later wave of
266 downregulation, initiated from 17 to 19 DAA, included the C2C2 GATA, GARP G2-like, and MADS_II
267 families. Similar to upregulation of TFs, the downregulation tended to continue throughout the rest
268 of the timecourse, indicating a gradual change in TF expression levels. None of the TF families were
269 significantly enriched for downregulated genes compared to all genes. These results differ from
270 Arabidopsis, where several families (C2C2-CO-like and TCP) were significantly enriched for
271 downregulated genes (Breeze et al., 2011).

272 These two waves of TF differential expression are analogous to the two waves of differential
273 expression observed for all gene classes (Fig. 1). This is consistent with TF roles as activators and

repressors of gene expression. These results suggest that specific TF families initiate temporally distinct changes in gene expression, broadly classed into an initial (3 to 7 DAA) and later (13 to 19 DAA) response.

Understand regulation using network modelling

Our results indicate that there are two main temporal waves of expression during senescence (from 3 to 7 DAA and from 13 to 19 DAA) that may be regulated by the associated up and downregulation of particular TF families. However, to understand the interactions between TFs and predict which ones may be key regulators (hub genes) driving this transcriptional programme, we constructed a gene regulatory network. We used Causal Structure Inference (Penfold and Wild, 2011), which produces a directional network of TF interactions. We used the 341 TFs that were differentially expressed during the timecourse to build the network.

To interpret the network it is necessary to determine the 'edge weight threshold' at which to include edges. Since our aim was to identify the most important TFs within the network to test as candidate genes for the regulation of senescence, we decided to compare the network across different edge weight thresholds. We hypothesised that by identifying TFs which were important across multiple thresholds, we would be more likely to identify robust candidate genes. We found that from an edge weight threshold of 0.01 to 0.3, the number of edges decreased from 12,832 to 61 (Table 1). *NAM-A1*, a known regulator of senescence in wheat, was only present in the network at the lower thresholds of 0.01, 0.05, and 0.1. We therefore decided to focus on the networks that included *NAM-A1*, as it is likely that the more stringent thresholds (0.2 and 0.3) would also have excluded other TFs relevant to the senescence process. The other TF which had previously been identified to regulate senescence in wheat (*NAC-S*) was not detected as differentially expressed during our timecourse so it was not used to construct the network or determine appropriate thresholds.

We determined the importance of a gene within the network using two measures: 'degree' which is the number of direct connections to other genes, and 'betweenness centrality' which is a measure of the number of shortest paths which pass through that gene and represents a measure of how essential the gene is to the flow of information around the network. We calculated percentage rankings of genes in each of the three edge weight thresholds that included *NAM-A1* (0.01, 0.05, and 0.1) according to their degree and betweenness centrality to allow comparison across networks with different numbers of genes (Supplemental Table S7).

Differentiating between top ranked candidate genes using complementary datasets

We hypothesised that TFs which were ranked highly in at least one threshold for degree and one threshold for betweenness centrality would represent good candidate genes for further investigation.

To explore this, we selected the TFs which were ranked in the top 5%, 10%, 20%, and 30% in at least one threshold for degree and one threshold for betweenness centrality (Table 2; Supplemental Table S7). We evaluated these different top ranked candidate TFs using two additional datasets: 1) expression data from an independent experiment with 70 tissues/time points in the spring wheat cultivar Azhurnaya which included senescing leaves (Ramirez-Gonzalez et al., 2018) and 2) a GENIE3 network of predicted TF – target relationships from 850 independent expression samples (Ramirez-Gonzalez et al., 2018).

Across all four thresholds, a higher percentage of TFs were upregulated in senescing tissues in Azhurnaya (27.6% to 36.1%) than in the network as a whole (22.0%, Table 2). Similarly, a higher percentage of these top ranked TFs shared predicted target genes with *NAM-A1* in the GENIE3 network than in our network as a whole (ranging from 30.4% to 45.1%, compared to 20.1%, Table 2). The highest enrichments (36.1% for senescence expression and 45.1% for *NAM-A1* shared targets) were both observed when we selected the top 10% of TFs in the network ($p < 0.06$ and $p < 0.001$, Fisher's exact test). We also examined whether the predicted target genes from the GENIE3 network were enriched for senescence-related GO terms. In this case only the TFs in the top 20% and top 30% had more targets with senescence-related GO terms (8.0% and 8.9%, respectively) than TFs in the whole network (4.9%). We also noticed that *NAM-A1* did not have target genes in the GENIE3 network enriched for senescence GO terms, suggesting that this GO enrichment data may miss some relevant candidate genes. Nevertheless, together these complementary data sources show that ranking the genes within a CSI network by degree and betweenness centrality can be an effective strategy to narrow down a candidate gene list.

The top 10% of TFs in the network were most likely to be upregulated during senescence in Azhurnaya and to share predicted downstream targets with *NAM-A1*, therefore we considered these to represent good candidate genes for further investigation. More stringent thresholds (top 5% of TFs) failed to increase the enrichment of senescence-related TFs, and indeed failed to include *NAM-A1* which is a known regulator of senescence. This highlights that the threshold chosen must be integrated with biological knowledge to ensure it remains biologically relevant.

Amongst the 36 top ranked genes (top 10% threshold), we found that three TF families were enriched compared to all 341 TFs in the network: GRAS, HSF, and RWP-RK ($\chi^2 < 0.001$, 0.01, and 0.05 respectively). Interestingly the RWP-RK family was also significantly enriched for upregulation during senescence (Fig. 3A), in addition to being enriched amongst top ranked genes in the network.

Using the information from the other datasets mentioned above (Azhurnaya expression and GENIE3 network) we found that 13 out of the 36 top ranked genes from the network were expressed over

two-fold higher in senescing tissues than in other tissues across the Azhurnaya developmental experiment (Fig. 4A). This independent dataset suggests that these 13 genes may play a specific role in senescing tissues and we hypothesise that they would be less likely to induce pleiotropic effects when their expression is altered in mutant or transgenic lines. We examined the function of the orthologs of all 36 top ranked candidate genes in Arabidopsis and rice (Supplemental Table S7), but only four of them had reported leaf senescence phenotypes in Arabidopsis, and none had senescence phenotypes in rice. This supports the low conservation of ortholog function across species. Using the independent GENIE3 TF - target network, we tested whether the 36 top ranked candidate genes had any shared target genes with *NAM-A1*, which might indicate they act together in the same senescence-related pathway. We found that 14 genes had one or more shared target genes with *NAM-A1* (Fig. 4B), and several of these were also upregulated in senescing Azhurnaya tissues (Fig. 4A). Even an overlap of one target gene is significantly more than the expected zero overlap between *NAM-A1* and a random TF (Sign test, $p < 0.001$). We found that only three of the candidate genes were direct targets of *NAM-A1* in the GENIE3 network, and these included *NAM-D1*, the D-genome homoeolog of *NAM-A1*, and *NAM-A2* and *NAM-D2*, paralogs of *NAM-A1* located on different chromosomes.

Validation of candidate gene *NAM-A2*

Using the additional information sources above, we selected *NAM-A2* (*TraesCS2A02G201800*) for phenotypic characterisation in wheat because it was amongst our 36 top ranked candidate genes, was upregulated in senescing leaves, and shared many downstream target genes with *NAM-A1*. Furthermore, the *NAM-A2* homoeologs *NAM-B2* (*TraesCS2B02G228900*) and *NAM-D2* (*TraesCS2D02G214100*) were also amongst the top 36 candidate genes. *NAM-A2* is a paralog of *NAM-A1* which regulates senescence and nutrient remobilisation (Avni et al., 2014; Harrington et al., 2019; Uauy et al., 2006). The homoeolog of *NAM-A2*, *NAM-B2*, was previously found to cause a slight delay in senescence (Pearce et al., 2014), but *NAM-A2* has not been previously characterised so was a strong candidate TF that might regulate senescence.

To test the predictions of our model, we identified TILLING mutations in *NAM-A2* and *NAM-B2* in a tetraploid Kronos background (Uauy et al., 2009; Krasileva et al., 2017). Due to the potential redundancy between homoeologs in wheat (Borrill et al., 2015b), we decided to generate double *NAM-A2*/*NAM-B2* mutants through crossing. We identified a mutation leading to a premature stop codon in *NAM-B2* (R170*; between subdomains D and E of the NAC domain (Kikuchi et al., 2000)), which is predicted to abolish protein function by creating a truncated protein lacking part of the NAC DNA-binding domain. For *NAM-A2*, we could not identify any mutations which would cause truncations, so instead we selected three missense mutations that were in highly conserved domains and were thus expected to play important roles in protein function (Fig. 5A), as has recently been

shown for *NAM-A1* (Harrington et al., 2019). These were located in the A, C, and D NAC subdomain and were predicted to be highly deleterious according to SIFT (Ng and Henikoff, 2003) and PSSM scores for the NAM family (pfam02365) (Marchler-Bauer et al., 2017). We crossed each of the *NAM-A2* missense mutants to the *NAM-B2* truncation mutant to create segregating populations from which wild type, single and double mutants were phenotyped in the F_3 generation.

Across the three populations with different missense mutations in *NAM-A2*, and a common truncation mutation in *NAM-B2*, there was a significant delay of 4.9 days in flag leaf senescence in the double mutant compared to wild type (padj <0.01, ANOVA post-hoc Tukey HSD; Fig. 5B-C). There were no significant differences between the single mutants and wild type in flag leaf senescence. Peduncle senescence was significantly delayed by 7.4 days in the double mutant compared to wild type (padj <0.001, ANOVA post-hoc Tukey HSD; Fig. 5D). In addition, the single A mutant was significantly later in peduncle senescence than wild type (3.9 days, padj <0.001, ANOVA post-hoc Tukey HSD). The single B mutant was not significantly different from wild type suggesting that the A genome homoeolog has a stronger effect on senescence than the B genome homoeolog. Since the comparison is between different types of mutations (missense compared to a truncation mutation) interpretation of the relative magnitudes is difficult, although the truncation mutation in the B genome would have been expected to produce at least an equivalent effect to the missense mutation in the A genome. These effects were largely consistent across the three different missense mutations, although the mutation in subdomain C (G111R) had the largest effect when combined into a double mutant compared to wild type (Supplemental Fig. S4).

Discussion

In this work, we have characterised the transcriptional processes associated with senescence in the wheat flag leaf. We found that specific TF families are associated with these changes in transcription and have used gene regulatory network modelling, alongside additional complementary information, to identify candidate genes controlling this process. We confirmed that one of these genes, *NAM-A2*, plays a role in senescence in wheat.

Time-resolved transcriptional control of senescence in wheat

We found that although 52,905 genes were expressed in senescing flag leaves, only 9,533 genes were differentially expressed during this time period. Sampling ten time points allowed us to observe that these 9,533 DEGs were largely divided into two temporal waves of transcriptional changes which may not have been captured using a less time-resolved set of data. Frequent sampling has also proven informative in other time-dependent processes in wheat, such as pathogen infection (Dobon et al., 2016), and represents a powerful approach to understand the co-ordination and regulation of gene expression changes throughout development and environmental responses (Bar-Joseph et al., 2012; Lavarenne et al., 2018).

We found that during the first wave of transcriptional changes, the majority of DEGs were downregulated, and these groups were enriched for GO terms related to translation, photosynthesis and amino acid biosynthesis. During the second wave, genes started to be upregulated with enrichment for GO terms related to vesicle mediated transport, protein transport, and phosphate transport. The chronology of biological processes is well conserved with Arabidopsis. For example, early downregulation of chlorophyll-related genes is observed in both Arabidopsis (Breeze et al., 2011) and wheat, whilst transport processes are upregulated later during senescence. The temporal order of senescence-related processes is also broadly conserved in maize although only three time points were sampled making fine-grain comparisons difficult (Zhang et al., 2014). In rice, a longer timecourse of flag leaf senescence has been studied (Lee et al., 2017), where the authors mainly focused on comparing flag leaf and second leaf senescence; nevertheless broadly similar processes were observed in both senescing rice leaves and the wheat flag leaf.

To test whether the conservation of biological processes during senescence between plant species is controlled by orthologous genes, we examined the expression profiles of wheat orthologs of Arabidopsis and rice senescence-related genes. We found that the expression profiles of wheat and rice genes were conserved more frequently than those of Arabidopsis and wheat genes, although even between the monocots (i.e. rice and wheat), only 65% of orthologs had similar expression profiles.

This result suggests that individual genes' functions may not be well conserved between species, although similar gene families are involved. These results are consistent with results from experiments studying flowering time, in which similar gene families were co-opted to regulate flowering time in both monocots and dicots, although the individual genes' functions and their interactions are re-arranged (Li and Dubcovsky, 2008).

The importance of TFs in tightly coordinating transcriptional changes during senescence is well known from other plant species (Podzimska-Sroka et al., 2015; Woo et al., 2016). We found that particular TF families were up and downregulated in two distinct waves, an initial and later response, following the pattern for all DEGs. We found that three TF families were enriched for upregulated genes during senescence at early (CCAAT_HAP2 and RWP-RK) and late (NAC) stages. Members of the NAC family have been characterised to play a role in regulating senescence in both wheat (Uauy et al., 2006; Zhao et al., 2015) and other plant species (Podzimska-Sroka et al., 2015). The CCAAT_HAP2 (NF-YA) family is less well characterised in this process, but one member has been shown to delay nitrate-induced senescence in Arabidopsis (Leyva-González et al., 2012) and the family was found to be enriched for genes upregulated during Arabidopsis senescence (Breeze et al., 2011) suggesting a potential conserved role. The RWP-RK family is known in Arabidopsis to control nitrogen responses (Chardin et al., 2014), and in cereals nitrogen remobilisation is closely connected with senescence, highlighting the potential for further investigations into this family in the future. Surprisingly, the WRKY TF family, which has been reported to play important roles in senescence in several other species such as Arabidopsis (Breeze et al., 2011; Woo et al., 2013), cotton (Lin et al., 2015), and soybean (Brown and Hudson, 2017), was not enriched for upregulation during senescence in wheat. It is possible that relatively few members of the WRKY family function in regulating senescence in wheat or that the function of WRKY TFs has diverged between wheat and other plant species. This potential for divergence in the regulation of senescence between species is supported by experiments characterising the rice ortholog of *NAM-B1*. Whilst the *NAM-B1* TF in wheat regulates monocarpic senescence (Uauy et al., 2006), the ortholog in rice (*Os07g37920*) regulates anther dehiscence and does not affect monocarpic senescence (Distelfeld et al., 2012).

Identifying candidate genes in networks

One of the aims of this study was to identify TFs which regulate the process of senescence. The rationale behind this approach was that TFs control other genes and therefore may have a strong and readily detectable effect on the process of senescence. Secondly, in crops, TFs have been frequently selected under quantitative trait loci for important traits such as flowering time (*PPD1*, *VRN1*) (Yan et al., 2003; Beales et al., 2007) and cold tolerance (*CBF*) (Knox et al., 2008) due to their strong phenotypic

effects. Thus, identified candidate TFs regulating senescence might also prove to be useful breeding targets.

Through examining the expression patterns of TFs in detail, we identified TF families which were enriched for upregulation during senescence, however this analysis cannot provide information about which of the individual TFs within the family might be more important in regulating the senescence process. To address this question, we used Causal Structure Inference (Penfold and Wild, 2011) to identify interactions between TFs. Our hypothesis was that central transcriptional regulators of senescence would regulate other TFs to create a regulatory cascade to influence the thousands of genes differentially expressed during senescence. We found that the most highly ranked candidate genes from the network were enriched for senescence-related functions compared to all genes within the network. We therefore propose that the ranking of candidate genes based on degree and betweenness centrality can be a practical strategy to narrow down long lists of candidate genes from network analyses.

Amongst the 36 top ranked TFs in the network, three TF families were enriched: GRAS, HSF, and RWP-RK. Members of the GRAS family play diverse roles in plant development, and in particular the DELLA subfamily has been reported to play a role in senescence in Arabidopsis (Chen et al., 2014). HSF TFs are associated with stress responses, and although no members have been associated with developmental senescence, stress-responsive genes are also closely associated with environmentally-induced senescence, and common regulation has been observed in Arabidopsis (Woo et al., 2013). The RWP-RK family is of interest because it is also significantly enriched for upregulation during senescence, in addition to being enriched amongst top ranked genes in the network. This adds further weight to the hypothesis that the RWP-RK TFs may play a role in senescence, in addition to their known role in nitrogen responses (Chardin et al., 2014). The roles of these identified TFs can now be directly tested in wheat to determine whether they regulate senescence using gene editing and TILLING (Borrill et al., 2019).

To further delimit this list of candidate genes, we used information from independent datasets (developmental timecourse of expression and GENIE3 TF-target network) to prioritise candidate genes. The approach to combine additional data sets was also applied in Arabidopsis where a Y1H screen was used in conjunction with Causal Structure Inference to help to identify regulatory interactions in senescence and pathogen infection (Hickman et al., 2013). Another approach that can be used to narrow down candidate genes is to examine how the network is perturbed in TF mutants. This approach was used in Arabidopsis to identify three NAC TFs which regulate senescence (Kim et

al., 2018) and could now be applied in wheat using the TILLING mutant resource (Krasileva et al., 2017), for example starting with the mutants generated in this study.

To test the predicted function of these candidate genes in regulating wheat senescence, we focused on *NAM-A2*, which is a paralog of the known *NAM-B1* gene (Uauy et al., 2006). We found significant delays in flag leaf and peduncle senescence in *NAM-A2/NAM-B2* double mutants, indicating that the genes predicted by the network play roles in senescence. The peduncle senescence phenotype indicates that this approach can identify genes that regulate senescence across different tissues, not only in the flag leaf, and may reflect that monocarpic senescence in wheat is a developmental process regulated across the whole plant (Harrington et al., 2019). Ongoing work is currently characterising the additional candidate genes through the development of wheat double mutants for phenotypic characterisation.

Future directions

This study has uncovered candidate TFs that may regulate senescence in wheat and has confirmed the role of one of these genes in regulating senescence. It will be of great interest to determine whether these genes only control senescence or also affect nutrient remobilisation and hence influence final grain nutrient content. In addition to deepening our understanding of the molecular regulation of senescence, this study lays the groundwork to use this network-enabled approach to identify TFs regulating a range of different biological processes which happen across a timecourse. This approach is not only applicable to developmental processes but could equally be applied to abiotic and biotic stresses, as has been carried out in other plant species (Hickman et al., 2013). This approach could also be applied to identify candidate genes for traits in species without genome sequences, although a transcriptome would need to be assembled from the RNA-Seq data. The advent of genome-editing means that the prediction of gene function could readily be tested in any transformable species.

Conclusion

The availability of a fully sequenced reference genome for wheat, alongside functional genomic resources such as the TILLING population, have brought wheat biology into the genomics era and have made possible studies which even a few years ago would have been unthinkable. Here we have used these new resources to characterise the transcriptional processes occurring during wheat senescence. We found that specific TF families are associated with this process in wheat, some of which have been reported in other species, but others present new links between TF families and the process of senescence. Although these associations do not prove causality, the hypotheses generated can now

be tested experimentally in wheat using TILLING or gene editing. Gene network modelling, when used in conjunction with complementary datasets, is a powerful approach that can accelerate the discovery of genes regulating biological processes in both model and crop species.

Methods

Plant growth for RNA-Seq timecourse

We pre-germinated seeds of hexaploid wheat cv. Bobwhite on moist filter paper for 48 h at 4°C followed by 48 h in the dark at room temperature (~20°C). These pre-germinated seeds were sown in P40 trays in 85% fine peat with 15% horticultural grit. Plants were potted on at 2–3 leaf stage to 1L square pots with 1 plant per pot in Petersfield Cereal Mix (Petersfield, Leicester, UK). Plants were grown in 16 h light at 20°C, with 8 h dark at 15°C. The main tiller was tagged at anthesis, and the anthesis date was recorded.

Phenotyping for RNA-Seq timecourse

We measured the chlorophyll content of flag leaves across the timecourse from 3 to 26 days after anthesis (DAA) using a SPAD-502 chlorophyll meter (Konica Minolta). The time points used were 3, 7, 10, 13, 15, 17, 19, 21, 23, and 26 DAA. We measured the flag leaf from the main tiller (tagged at anthesis) for five separate plants for each time point, taking measurements at eight different locations distributed along the length of each flag leaf. Three of these measured leaves were subsequently harvested for RNA extraction.

We measured the grain moisture content across the timecourse from 3 to 26 days after anthesis, using the same time points as for chlorophyll measurements. We harvested eight grains from central spikelets (floret positions 1 and 2) within the primary spike of five separate plants at each time point, these grains were weighed, and then dried at 65°C for 72 hours before re-weighing. The difference in weight was used to calculate the percentage grain moisture content.

Tissue harvest, RNA extraction and sequencing

Harvesting

The flag leaf from the main tiller was harvested at 3, 7, 10, 13, 15, 17, 19, 21, 23, and 26 DAA from three separate plants (three biological replicates). We harvested the middle 3 cm of the flag leaf lengthways to have a region of the leaf which was synchronised in its developmental stage. We flash froze the samples in liquid nitrogen, then stored them at -80°C prior to processing. In total we harvested 30 samples.

RNA extraction

We ground the samples to a fine powder in mortar and pestles which had been pre-chilled with liquid nitrogen. We extracted RNA using Trizol (ThermoFisher) according to the manufacturer's instructions, using 100 mg ground flag leaf per 1 ml Trizol. We removed genomic DNA contamination using DNAseI (Qiagen) according to the manufacturer's instructions and cleaned up the samples using the RNeasy Mini Kit (Qiagen) according to the manufacturer's instructions.

Library preparation

The quality of the RNA was checked using a Tecan plate reader with the Quant-iT™ RNA Assay Kit (Life technologies/Invitrogen Q-33140) and also the Quant-iT™ DNA Assay Kit, high sensitivity (Life technologies/Invitrogen Q-33120). Finally the quality of the RNA was established using the PerkinElmer GX with a high sensitivity chip and High Sensitivity DNA reagents (PerkinElmer 5067-4626). 30 Illumina TruSeq RNA libraries were constructed on the PerkinElmer Sciclone using the TruSeq RNA protocol v2 (Illumina 15026495 Rev.F). After adaptor ligation, the libraries were size selected using Beckman Coulter XP beads (Beckman Coulter A63880). This removed the majority of un-ligated adapters, as well as any adapters that may have ligated to one another. The PCR was performed with a primer cocktail that annealed to the ends of the adapter to enrich DNA fragments that had adaptor molecules on both ends. The insert size of the libraries was verified by running an aliquot of the DNA library on a PerkinElmer GX using the High Sensitivity DNA chip and reagents (PerkinElmer CLS760672) and the concentration was determined by using the Tecan plate reader.

Sequencing

The TruSeq RNA libraries were normalised and equimolar pooled into one final pool using elution buffer (Qiagen). The library pool was diluted to 2 nM with NaOH and 5 µL transferred into 995 µL HT1 (Illumina) to give a final concentration of 10 pM. 120 µL of the diluted library pool was then transferred into a 200 µL strip tube, spiked with 1% v/v PhiX Control v3 and placed on ice before loading onto the Illumina cBot. The flow cell was clustered using HiSeq PE Cluster Kit v3, utilising the Illumina PE_Amp_Lin_Block_Hyb_V8.0 method on the Illumina cBot. Following the clustering procedure, the flow cell was loaded onto the Illumina HiSeq 2000/2500 instrument following the manufacturer's instructions. The sequencing chemistry used was HiSeq SBS Kit v3 with HiSeq Control Software 2.2.58 and RTA 1.18.64. Reads (100 bp, paired end) in bcl format were demultiplexed based on the 6bp Illumina index by CASAVA 1.8, allowing for a one base-pair mismatch per library, and converted to FASTQ format by bcl2fastq.

RNA-Seq data analysis

Mapping

We pseudoaligned the samples using kallisto v0.44.0 with default parameters to the RefSeqv1.0 annotation v1.1 (IWGSC et al., 2018). Transcripts per million (TPM) and counts for all samples were merged into a single dataframe using tximport v1.0.3 (Soneson et al., 2016). Scripts for data analysis are available from https://github.com/Borrill-Lab/WheatFlagLeafSenescence.

Differential expression analysis

We filtered for high confidence genes which were expressed on average > 0.5 TPM in at least one time point; this excluded low expressed genes and low confidence gene models from further analysis, consistent with previous analyses in wheat (Ramirez-Gonzalez et al., 2018). In total 52,905 genes met this condition. We used the count expression level of these genes for differential expression analysis using the R package ImpulseDE2 v1.4.0 (Fischer et al., 2018), all counts were rounded to the nearest integer before they were analysed with ImpulseDE2. In parallel we used the TPM expression level of these 52,905 genes for differential expression analysis using Gradient Tool v1.0 (Breeze et al., 2011) with the normalisation enabled on Cyverse (https://de.cyverse.org/de/) (Merchant et al., 2016). To select a high confidence set of DEGs we only retained genes which were differentially expressed padj < 0.001 from ImpulseDE2 and which were differentially expressed according to Gradient Tool with a z-score of >|2|. We grouped the 9,533 high confidence DEGs according to the first time point at which they were up or downregulated, according to Gradient Tool. The Gradient Tool uses Gaussian process regression to identify whether gene expression is increasing or decreasing at each time point (Breeze et al., 2011). For example, a gene first upregulated at 10 DAA was in group “U10” (up 10 DAA), whereas a gene first downregulated at this time point was assigned to group “D10” (down 10 DAA). Genes which were both up and downregulated during the timecourse (< 4% of all DEGs) were grouped according to the time point of first differential expression with the opposite change also indicated. For example a gene upregulated at 10 DAA and then downregulated at 15 DAA was grouped as U10D (the second time point of differential expression was not recorded in the grouping). These groupings are available in (Supplemental Table S2). The minority of genes with both up and downregulation (<4 % of all DEGs) were excluded from GO term enrichment analysis.

GO term enrichment

We obtained GO terms from the RefSeqv1.0 annotation and transferred them from the annotation v1.0 to v1.1. We only transferred GO terms for genes which shared > 99% identity across > 90% of the sequence (105,182 genes; 97.5% of all HC genes annotated in v1.1). GO term enrichment was carried

out for each group of DEGs (groups defined according to the first time point at which genes were upregulated or downregulated, see above) using GOseq v1.24.0.

Ortholog identification

We identified the rice and Arabidopsis orthologs of the wheat genes using *Ensembl*Plants ortholog information downloaded via BioMart (Kersey et al., 2018). Functional annotation for Supplemental Table S7 was obtained from funricegenes (Li et al., 2017), RAP-DB (Sakai et al., 2013), Araport (Cheng et al., 2017), and literature searches.

Arabidopsis and rice leaf senescence gene expression

Arabidopsis gene expression data during a timecourse of leaf senescence was obtained from Breeze et al. (2011). Gene expression patterns had already been assigned using Gradient Tool v1.0 by Breeze et al. (2011). Rice gene expression data for a timecourse of flag leaf senescence were obtained from Lee et al. (2017). Gene expression data was presented in this publication as the $\log_2$ normalised read count for each time point compared to expression level at the initial time point (4 days after heading). The gradient tool had not been used on this dataset therefore we assigned a general trend in expression (increasing or decreasing according to the $\log_2$ fold change) for time points up to 28 days after heading when the first loss of chlorophyll was observed (comparable to the end of our wheat senescence timecourse) (Supplemental Table S6).

TF annotation

Genes which were annotated as TFs were obtained from https://opendata.earlham.ac.uk/wheat/under_license/toronto/Ramirez-Gonzalez_etal_2018-06025-Transcriptome-Landscape/data/data_tables/ (Ramirez-Gonzalez et al., 2018).

Gene regulatory network construction

We selected the 341 TFs which were amongst the 9,533 DEGs. We used the TPM gene expression values as input to Causal Structure Inference (CSI) v1.0 (Penfold and Wild, 2011) which was run through Cyverse (https://de.cyverse.org/de/) (Merchant et al., 2016). The parameters used with CSI were the defaults (parental set depth =2, gaussian process prior = 10;0.1, weight truncation = 1.0E-5, data normalisation = standardise (zero mean, unit variance), weight sampling = FALSE). The output marginal file was converted to Cytoscape format using hCSI_MarginalThreshold v1.0 in Cyverse with a probability threshold of 0.01. We used this file for directed network analysis in Cytoscape v3.6.1 (Shannon et al., 2003) which produced network statistics. We used Cytoscape to filter the network for degree and betweenness centrality at 0.01, 0.05, 0.1, 0.2, and 0.3.

GENIE3 data

We identified the targets of TF using a TF-target network which was previously published (Ramirez-Gonzalez et al., 2018). Only connections amongst the top one million links were considered in this analysis. The network had been produced by a random forest approach (GENIE3) (Huynh-Thu et al., 2010) using 850 RNA-Seq samples.

Visualisation

Graphs were made in R using the packages ggplot2 (Wickham, 2016), NMF (aheatmap function) (Gaujoux and Seoighe, 2010), and pheatmap (Kolde, 2013).

Candidate gene validation

Phenotyping of NAM-2 *mutants*

We selected mutant lines from the Kronos TILLING population (K0282, K0427, K3240) (Krasileva et al., 2017) with missense mutations (G111R, G133D, P40S, respectively) in *NAM-A2* (*TraesCS2A02G201800*). These *NAM-A2* mutant lines were crossed with a line containing a mutation inducing a premature stop codon in *NAM-B2* (*TraesCS2B02G228900*) (K4452; R170*). For each of the three crosses, heterozygous F_1 seeds (AaBb) were self-pollinated to produce an F_2 population. We selected double homozygous mutant (aabb), single homozygous mutant (aaBB or AAbb), and double homozygous wild type plants (AABB) in the F_2 using KASP markers (Supplemental Table S8) as described in Ramirez-Gonzalez et al. (2015). Seeds from two individuals of each genotype in the F_2 population were grown in greenhouse conditions for phenotyping from Jan 2018 – May 2018 in Norwich with 16 h supplemental lighting and a daytime temperature of 18°C, and a night-time temperature of 12°C. For each genotype we tagged the main tiller at anthesis and recorded the anthesis date for 16-20 individual plants. We scored flag leaf senescence as the date when the flag leaf of the main tiller had lost chlorophyll from 25% of the flag leaf blade. We scored peduncle senescence as the date when the top 3 cm of the peduncle lost all green colour and turned straw-yellow.

Statistical analyses

Statistical analyses were carried out using the base R package. Statistical tests used and the number of samples are indicated in the appropriate figure legends.

Accession numbers

RNA-Seq raw reads have been deposited in the SRA accession PRJNA497810. The original TILLING mutant lines can be ordered from JIC Germplasm Resources Unit (https://www.seedstor.ac.uk/).

NAM-A2 is *TraesCS2A02G201800* in the RefSeqv1.1 gene annotation available from EnsemblPlants (https://plants.ensembl.org/Triticum_aestivum/Info/Index).

Acknowledgements

This work was supported by the UK Biotechnology and Biological Sciences Research Council (BBSRC) through an Anniversary Future Leader Fellowship to P.B. (BB/M014045/1) and the Designing Future Wheat (BB/P016855/1) and GEN (BB/P013511/1) ISPs. S.A.H. was supported by the John Innes Foundation. This research was also supported in part by the NBI Computing infrastructure for Science (CiS) group through the HPC resources.

Tables

Table 1. Comparing CSI network at different thresholds for edge weight.

Edge weight threshold	# TFs	# edges	*NAM-A1* included in network
0.01	341	12,832	Yes
0.05	295	843	Yes
0.1	190	277	Yes
0.2	99	109	No
0.3	64	61	No

Table 2. Evaluation of candidate TFs selected from the CSI network using independent data sources. We selected the TFs which were ranked in the top 5%, 10%, 20%, and 30% in at least one threshold for degree and one threshold for betweenness centrality as potential candidate genes for further investigation. Independent data sources were used to determine whether these top candidate genes were enriched for TFs which 1) were upregulated in independent gene expression data (Azhurnaya developmental timecourse), 2) had target genes predicted in a GENIE3 network which were shared with *NAM-A1*, and 3) had target genes predicted in a GENIE3 network which were enriched for senescence GO terms.

TF group	Number of TFs	*NAM-A1* included	Percentage of TFs upregulated 2x in Azhurnaya	Percentage of TFs with GENIE3 targets	Percentage of TFs with GENIE3 targets enriched for

				shared with *NAM-A1*	senescence GO terms
Entire network	341	Yes	22.0	20.1	4.9
Top 30%	140	Yes	28.6	30.4	8.9
Top 20%	105	Yes	27.6	34.0	8.0
Top 10%	36	Yes	36.1	45.1	3.2
Top 5%	15	No	33.3	33.3	0

701

Figures

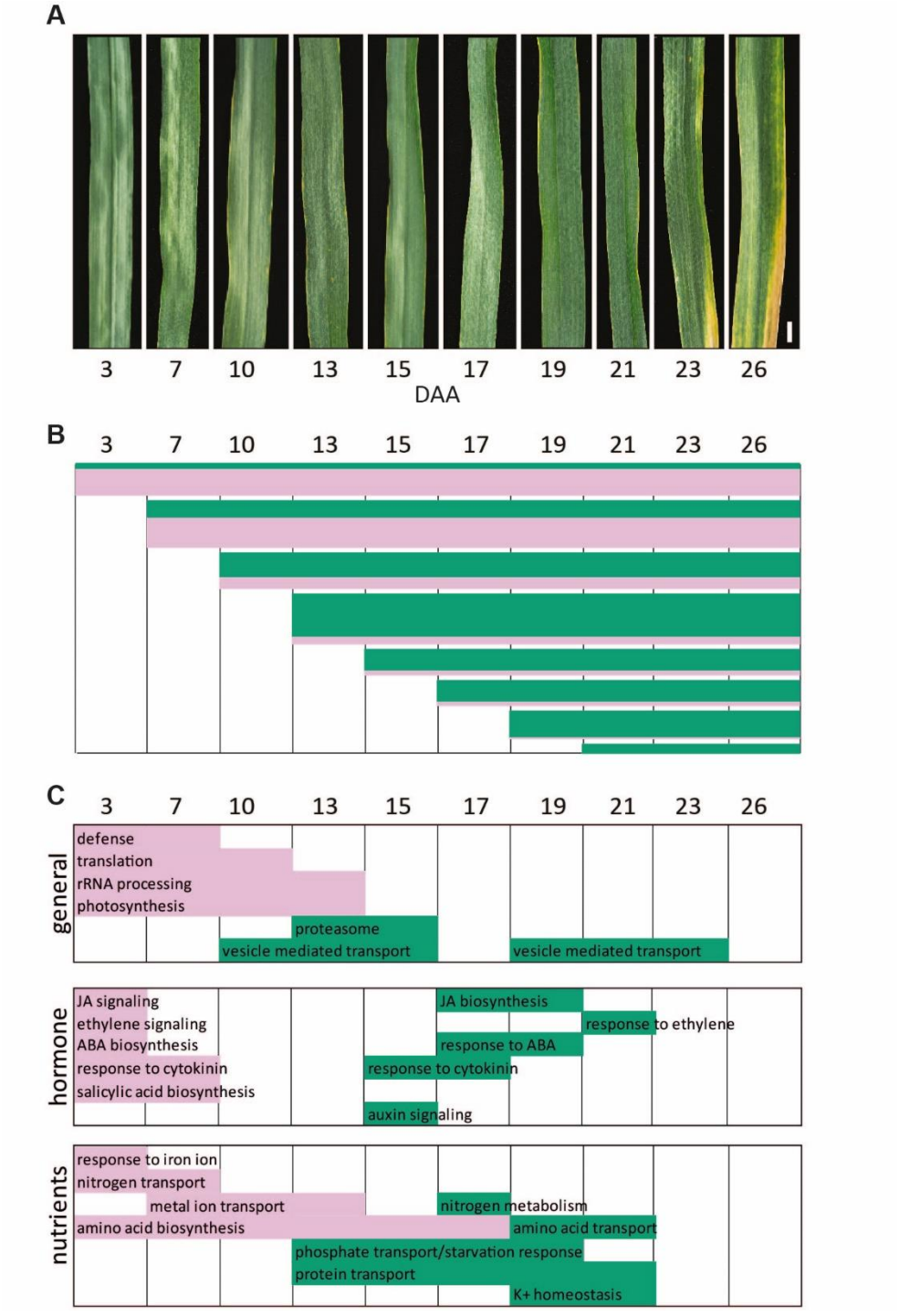

Figure 1. Transcriptional re-programming during flag leaf senescence. A) Timecourse of flag leaf senescence from 3 to 26 days after anthesis (DAA), scale bar represents 1 cm. B) Diagram showing representative patterns for genes which are consistently upregulated (green) or consistently downregulated (pink) during senescence (96.2% of DEGs). Genes were grouped according to the first time of up or downregulation. The majority of genes in each pattern continued to be up or downregulated across the whole timecourse. Bar heights represent the number of genes in each

expression pattern. The x axis represents time after anthesis, the axis is represented uniformly although time points are not evenly spaced. C) GO term enrichments are shown related to general, hormone and nutrient related processes. Filled rectangles represent that genes starting to be differentially expressed at that time point are enriched for that specific GO terms. Green rectangles represent upregulated genes, pink rectangles represent downregulated genes.

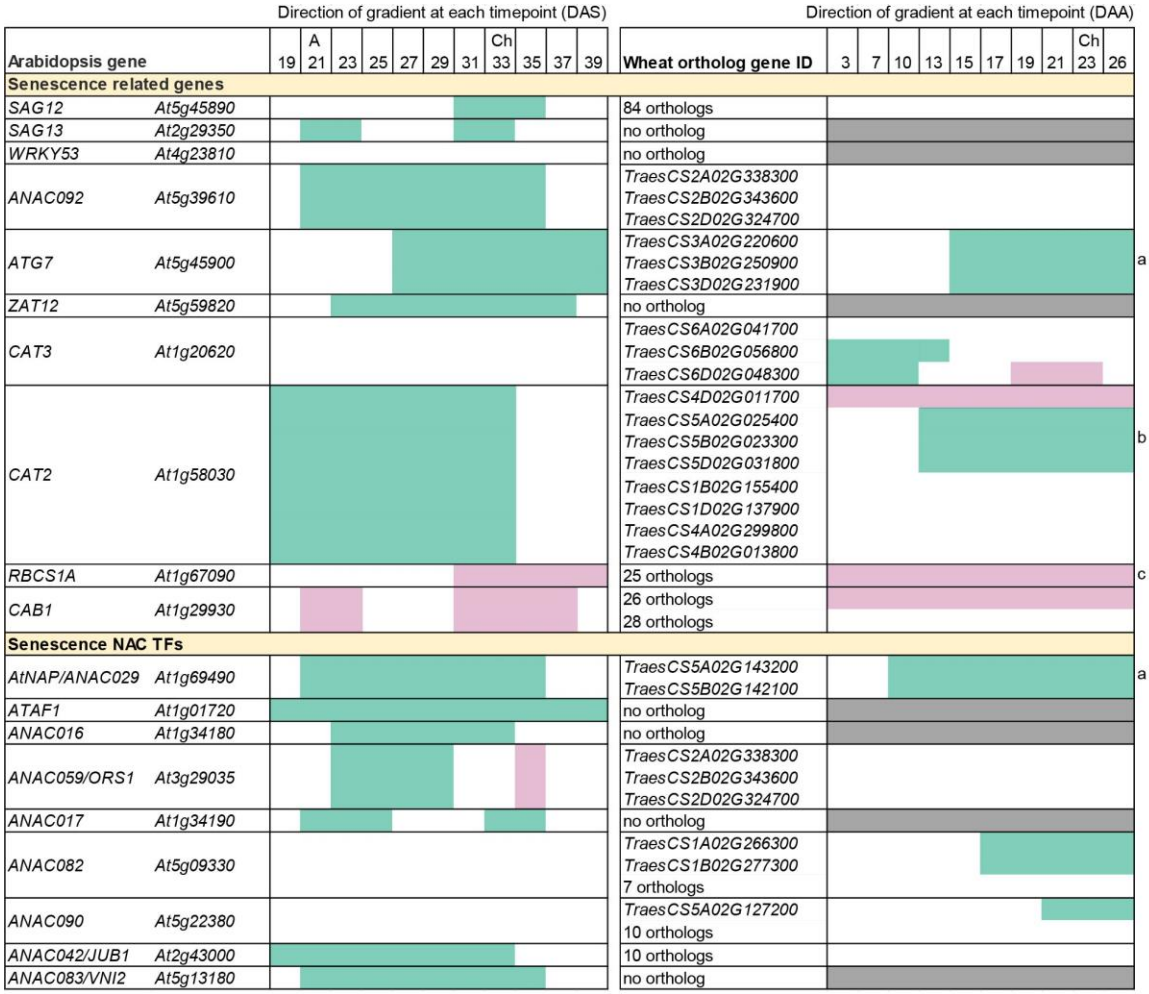

Figure 2. Expression profiles of Arabidopsis senescence-related genes and NAC transcription factors (left) and their wheat orthologs (right). The significant gradient changes are indicated over the course of an 11 time point timecourse in Arabidopsis (4th rosette leaf from 19 to 39 days after sowing (DAS), Breeze et al., 2011) and over a 10 time point timecourse in wheat (flag leaf from 3 to 26 days after anthesis (DAA), this study, see Figure S3). The 21 DAS time point in the Arabidopsis data corresponds to anthesis (A), equivalent to 0 DAA for the wheat data. Likewise, the first visible loss of chlorophyll (Ch) occurs at 33 DAS and 23 DAA, respectively (see Figure S3). The direction of the gradient at each time point is highlighted as either upregulated (green) or downregulated (pink). Cells in white indicate there was no change at this time point. Grey cells indicate that no wheat ortholog was identified. One wheat ortholog is represented per row, except where five or more wheat orthologs with the same pattern of expression were identified, for clarity these are represented within a single row. a Representative pattern shown, full details in Table S4. b Representative pattern shown for chromosome 5 homoeologs, full details in Table S4. c 23 out of 25 orthologs were DE, all with this pattern.

Figure 2. Expression profiles of Arabidopsis senescence-related genes and NAC transcription factors (left) and their wheat orthologs (right). The significant gradient changes are indicated over the course of an 11 time point timecourse in Arabidopsis (4th rosette leaf from 19 to 39 days after sowing (DAS), Breeze et al., 2011) and over a 10 time point timecourse in wheat (flag leaf from 3 to 26 days after

anthesis (DAA), this study, see Figure S3). The 21 DAS time point in the Arabidopsis data corresponds to anthesis (A), equivalent to 0 DAA for the wheat data. Likewise, the first visible loss of chlorophyll (Ch) occurs at 33 DAS and 23 DAA, respectively (see Figure S3). The direction of the gradient at each time point is highlighted as either upregulated (green) or downregulated (pink). Cells in white indicate there was no change at this time point. Grey cells indicate that no wheat ortholog was identified. One wheat ortholog is represented per row, except where five or more wheat orthologs with the same pattern of expression were identified, for clarity these are represented within a single row. [a] Representative pattern shown, full details in Supplemental Table S4. [b] Representative pattern shown for chromosome 5 homoeologs, full details in Supplemental Table S4. [c] 23 out of 25 orthologs were DE, all with this pattern.

730

731 **Figure 3. Percentage of expressed genes which were differentially expressed per transcription factor**
732 **family at each time point.** Upregulated (A) and downregulated (B) genes are shown. The total number
733 of genes expressed in each family is shown in brackets after the family name. Time points during which
734 specific transcription factor families which were significantly enriched for upregulation are indicated
735 with asterisks (* = $p < 0.05$, ** = $p < 0.01$). No families were significantly enriched for downregulation.

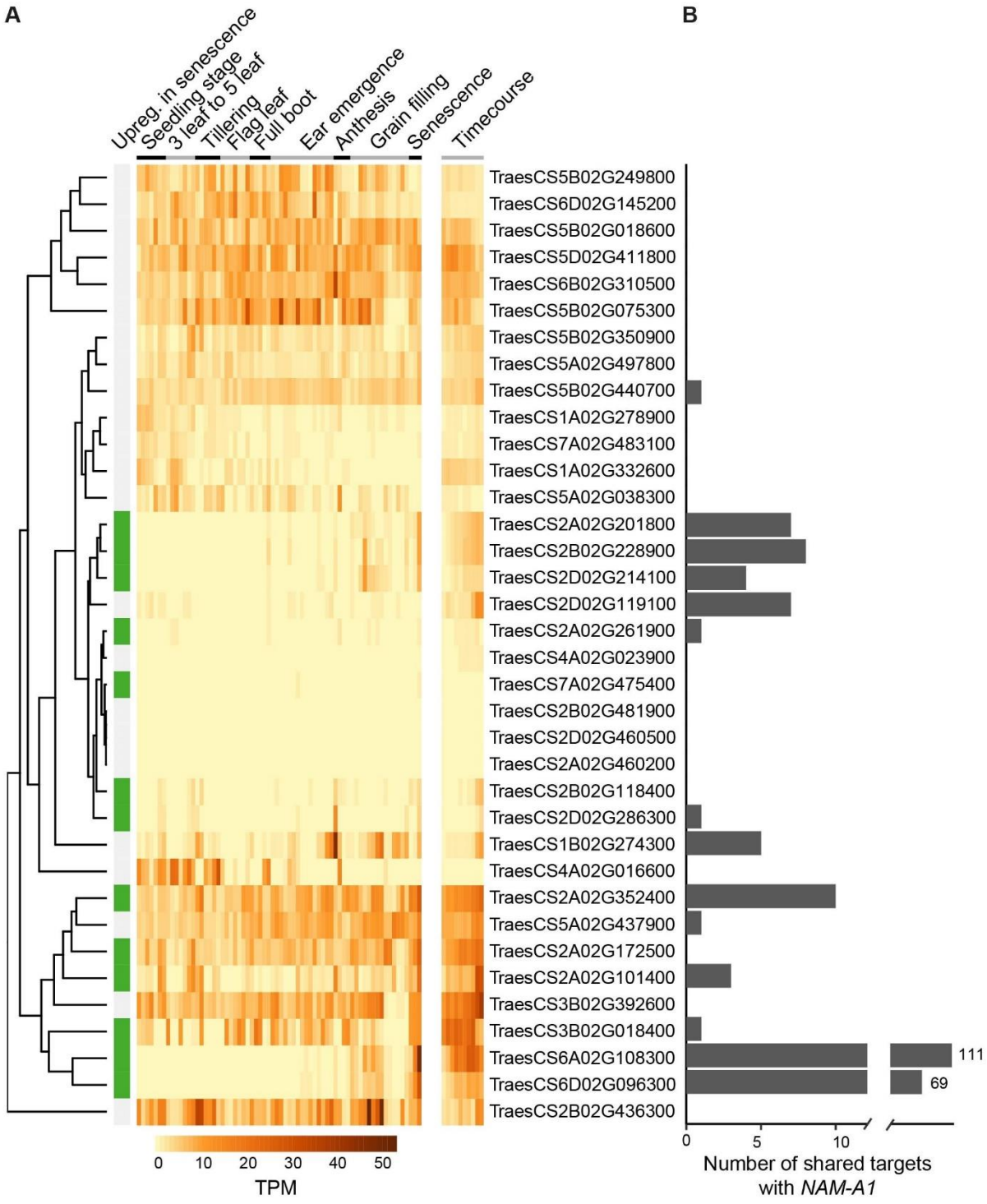

Figure 4. Additional information for 36 top ranked candidate genes. A) Expression from an independent RNA-Seq experiment using Azhurnaya spring wheat (left part of heatmap) and expression in the senescence timecourse (right part of heatmap, "Timecourse"). Each of the 36 genes is represented in one row, and rows are sorted according to the similarity of the expression patterns (dendrogram to left). Expression level is measured in transcripts per million (TPM). Genes which were over two-fold upregulated in senescence compared to other tissues/time points in Azhurnaya are highlighted by green boxes in the left-hand column ("Upreg. in senescence"). B) The number of targets

each transcription factor shares with *NAM-A1*, predicted by the independent GENIE3 network. *NAM-A1* (*TraesCS6A02G108300*) has 111 targets and its homoeolog *NAM-D1* (*TraesCS6D02G096300*) has 69 shared targets, shown with broken axis.

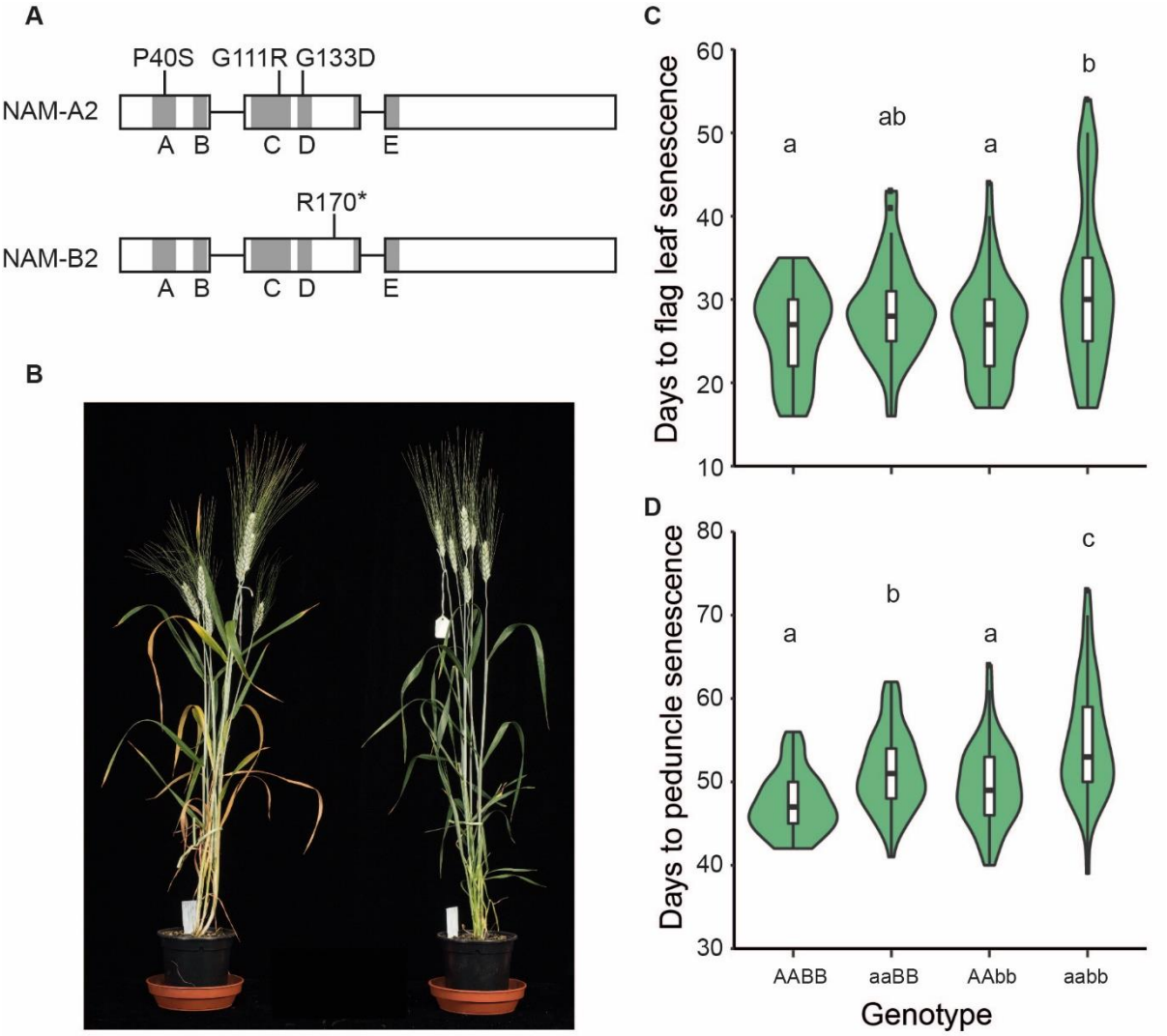

Figure 5. Mutants in *NAM-A2* and *NAM-B2*. A) Selected missense mutations in *NAM-A2* and stop mutation in *NAM-B2*. Grey regions are the NAC subdomains A-E. Subdomain E spans the end of exon 2 and the start of exon 3. B) Wild type sister line (left) and *NAM-A2 NAM-B2* double homozygous (aabb) mutant (right), 37 days after anthesis. C) Days from heading to flag leaf senescence and D) days from heading to peduncle senescence in wild type, single and double mutants across all three populations (different missense mutation in *NAM-A2*, common truncation mutation in *NAM-B2*). Letters indicate significant differences $p < 0.05$, with ANOVA post-hoc Tukey HSD, n = 53-61 individual plants per genotype. The populations are shown separately in Supplemental Figure S4.

Supplemental Data

The following supplemental materials are available.

Supplemental Figure S1. SPAD chlorophyll meter readings for flag leaves across the timecourse.

Supplemental Figure S2. Grain moisture content across the timecourse.

Supplemental Figure S3. Comparison of senescence progress in wheat and Arabidopsis leaves.

Supplemental Figure S4. Senescence phenotypes of individual missense mutations in *NAM-A2*.

Supplemental Table S1. Total number of reads and pseudoaligned reads per sample.

Supplemental Table S2. The 9,533 genes differentially expressed during senescence.

Supplemental Table S3. GO terms enriched per grouped expression pattern.

Supplemental Table S4. Wheat orthologs of Arabidopsis senescence-related genes.

Supplemental Table S5. Wheat orthologs of senescence-related rice genes.

Supplemental Table S6. Expression patterns of wheat orthologs and senescence-related rice genes.

Supplemental Table S7. The 341 transcription factors in the CSI network with additional information.

Supplemental Table S8. Primers used for KASP genotyping of *NAM-2* mutants.

References

Avni, R., Zhao, R., Pearce, S., Jun, Y., Uauy, C., Tabbita, F., Fahima, T., Slade, A., Dubcovsky, J., and Distelfeld, A. (2014). Functional characterization of *GPC-1* genes in hexaploid wheat. Planta *239*, 313-324.

Balazadeh, S., Kwasniewski, M., Caldana, C., Mehrnia, M., Zanor, M.I., Xue, G.-P., and Mueller-Roeber, B. (2011). *ORS1*, an H_2O_2-responsive NAC transcription factor, controls senescence in Arabidopsis thaliana. Molecular plant *4*, 346-360.

Bar-Joseph, Z., Gitter, A., and Simon, I. (2012). Studying and modelling dynamic biological processes using time-series gene expression data. Nature Reviews Genetics *13*, 552.

Beales, J., Turner, A., Griffiths, S., Snape, J.W., and Laurie, D.A. (2007). A *Pseudo-Response Regulator* is misexpressed in the photoperiod insensitive *Ppd-D1a* mutant of wheat (*Triticum aestivum* L.). Theoretical and Applied Genetics *115*, 721-733.

Borrill, P., Fahy, B., Smith, A.M., and Uauy, C. (2015a). Wheat Grain Filling Is Limited by Grain Filling Capacity rather than the Duration of Flag Leaf Photosynthesis: A Case Study Using *NAM* RNAi Plants. PLOS ONE *10*, e0134947.

Borrill, P., Adamski, N., and Uauy, C. (2015b). Genomics as the key to unlocking the polyploid potential of wheat. New Phytologist *208*, 1008-1022.
Borrill, P., Harrington, S.A., and Uauy, C. (2019). Applying the latest advances in genomics and phenomics for trait discovery in polyploid wheat. The Plant Journal *97*, 56-72.
Bowers, J.E., Chapman, B.A., Rong, J., and Paterson, A.H. (2003). Unravelling angiosperm genome evolution by phylogenetic analysis of chromosomal duplication events. Nature *422*, 433.
Bray, N.L., Pimentel, H., Melsted, P., and Pachter, L. (2016). Near-optimal probabilistic RNA-seq quantification. Nature biotechnology *34*, 525-527.
Breeze, E., Harrison, E., McHattie, S., Hughes, L., Hickman, R., Hill, C., Kiddle, S., Kim, Y.-s., Penfold, C.A., Jenkins, D*., et al.* (2011). High-Resolution Temporal Profiling of Transcripts during *Arabidopsis* Leaf Senescence Reveals a Distinct Chronology of Processes and Regulation. The Plant Cell *23*, 873-894.
Bresson, J., Bieker, S., Riester, L., Doll, J., and Zentgraf, U. (2017). A guideline for leaf senescence analyses: from quantification to physiological and molecular investigations. Journal of Experimental Botany *69*, 769-786.
Brown, A.V., and Hudson, K.A. (2017). Transcriptional profiling of mechanically and genetically sink-limited soybeans. Plant, Cell & Environment *40*, 2307-2318.
Buchanan-Wollaston, V., Earl, S., Harrison, E., Mathas, E., Navabpour, S., Page, T., and Pink, D. (2003). The molecular analysis of leaf senescence – a genomics approach. Plant Biotechnology Journal *1*, 3-22.
Chardin, C., Girin, T., Roudier, F., Meyer, C., and Krapp, A. (2014). The plant RWP-RK transcription factors: key regulators of nitrogen responses and of gametophyte development. Journal of Experimental Botany *65*, 5577-5587.
Charles, M., Tang, H., Belcram, H., Paterson, A., Gornicki, P., and Chalhoub, B. (2009). Sixty Million Years in Evolution of Soft Grain Trait in Grasses: Emergence of the Softness Locus in the Common Ancestor of Pooideae and Ehrhartoideae, after their Divergence from Panicoideae. Molecular Biology and Evolution *26*, 1651-1661.
Chen, M., Maodzeka, A., Zhou, L., Ali, E., Wang, Z., and Jiang, L. (2014). Removal of DELLA repression promotes leaf senescence in Arabidopsis. Plant Science *219-220*, 26-34.
Cheng, C.-Y., Krishnakumar, V., Chan, A.P., Thibaud-Nissen, F., Schobel, S., and Town, C.D. (2017). Araport11: a complete reannotation of the Arabidopsis thaliana reference genome. The Plant Journal *89*, 789-804.
Distelfeld, A., Avni, R., and Fischer, A.M. (2014). Senescence, nutrient remobilization, and yield in wheat and barley. Journal of Experimental Botany *65*, 3783-3798.
Distelfeld, A., Pearce, S.P., Avni, R., Scherer, B., Uauy, C., Piston, F., Slade, A., Zhao, R., and Dubcovsky, J. (2012). Divergent functions of orthologous NAC transcription factors in wheat and rice. Plant molecular biology *78*, 515-524.
Dobon, A., Bunting, D.C.E., Cabrera-Quio, L.E., Uauy, C., and Saunders, D.G.O. (2016). The host-pathogen interaction between wheat and yellow rust induces temporally coordinated waves of gene expression. BMC Genomics *17*, 380.
Fang, C., Zhang, H., Wan, J., Wu, Y., Li, K., Jin, C., Chen, W., Wang, S., Wang, W., Zhang, H*., et al.* (2016). Control of Leaf Senescence by an MeOH-Jasmonates Cascade that Is Epigenetically Regulated by *OsSRT1* in Rice. Molecular Plant *9*, 1366-1378.
Fischer, A.M. (2012). The Complex Regulation of Senescence. Critical Reviews in Plant Sciences *31*, 124-147.
Fischer, D.S., Theis, F.J., and Yosef, N. (2018). Impulse model-based differential expression analysis of time course sequencing data. Nucleic Acids Research *46*, e119.
Garnett, T.P., and Graham, R.D. (2005). Distribution and Remobilization of Iron and Copper in Wheat. Annals of Botany *95*, 817-826.
Gaujoux, R., and Seoighe, C. (2010). A flexible R package for nonnegative matrix factorization. BMC Bioinformatics *11*, 367.

838 Gregersen, P.L., Culetic, A., Boschian, L., and Krupinska, K. (2013). Plant senescence and crop
839 productivity. Plant molecular biology *82*, 603-622.
840 Gregersen, P.L., and Holm, P.B. (2007). Transcriptome analysis of senescence in the flag leaf of wheat
841 (Triticum aestivum L.). Plant Biotechnology Journal *5*, 192-206.
842 Guo, Y., and Gan, S. (2006). *AtNAP*, a NAC family transcription factor, has an important role in leaf
843 senescence. The Plant Journal *46*, 601-612.
844 Harrington, S.A., Overend, L.E., Cobo, N., Borrill, P., and Uauy, C. (2019). Conserved residues in the
845 wheat (*Triticum aestivum*) NAM-A1 NAC domain are required for protein binding and when mutated
846 lead to delayed peduncle and flag leaf senescence. bioRxiv, 573881.
847 Hickman, R., Hill, C., Penfold, C.A., Breeze, E., Bowden, L., Moore, J.D., Zhang, P., Jackson, A., Cooke,
848 E., Bewicke-Copley, F.*, et al.* (2013). A local regulatory network around three NAC transcription factors
849 in stress responses and senescence in Arabidopsis leaves. The Plant Journal *75*, 26-39.
850 Huynh-Thu, V.A., Irrthum, A., Wehenkel, L., and Geurts, P. (2010). Inferring Regulatory Networks from
851 Expression Data Using Tree-Based Methods. PLOS ONE *5*, e12776.
852 IWGSC, Appels, R., Eversole, K., Feuillet, C., Keller, B., Rogers, J., Stein, N., Pozniak, C.J., Stein, N.,
853 Choulet, F.*, et al.* (2018). Shifting the limits in wheat research and breeding using a fully annotated
854 reference genome. Science *361*.
855 Kersey, P.J., Allen, J.E., Allot, A., Barba, M., Boddu, S., Bolt, B.J., Carvalho-Silva, D., Christensen, M.,
856 Davis, P., Grabmueller, C.*, et al.* (2018). Ensembl Genomes 2018: an integrated omics infrastructure
857 for non-vertebrate species. Nucleic Acids Research *46*, D802-D808.
858 Kichey, T., Hirel, B., Heumez, E., Dubois, F., and Le Gouis, J. (2007). In winter wheat (*Triticum aestivum*
859 L.), post-anthesis nitrogen uptake and remobilisation to the grain correlates with agronomic traits and
860 nitrogen physiological markers. Field Crops Research *102*, 22-32.
861 Kikuchi, K., Ueguchi-Tanaka, M., Yoshida, K.T., Nagato, Y., Matsusoka, M., and Hirano, H.-Y. (2000).
862 Molecular analysis of the NAC gene family in rice. Molecular and General Genetics MGG *262*, 1047-
863 1051.
864 Kim, H.J., Park, J.-H., Kim, J., Kim, J.J., Hong, S., Kim, J., Kim, J.H., Woo, H.R., Hyeon, C., Lim, P.O.*, et al.*
865 (2018). Time-evolving genetic networks reveal a NAC troika that negatively regulates leaf senescence
866 in *Arabidopsis*. Proceedings of the National Academy of Sciences.
867 Kim, J.H., Woo, H.R., Kim, J., Lim, P.O., Lee, I.C., Choi, S.H., Hwang, D., and Nam, H.G. (2009). Trifurcate
868 Feed-Forward Regulation of Age-Dependent Cell Death Involving *miR164* in *Arabidopsis*. Science *323*,
869 1053-1057.
870 Knox, A.K., Li, C., Vágújfalvi, A., Galiba, G., Stockinger, E.J., and Dubcovsky, J. (2008). Identification of
871 candidate CBF genes for the frost tolerance locus *Fr-A^{m}2* in *Triticum monococcum*. Plant molecular
872 biology *67*, 257-270.
873 Kolde, R. (2013). pheatmap: Pretty Heatmaps. . R package.
874 Krasileva, K.V., Vasquez-Gross, H.A., Howell, T., Bailey, P., Paraiso, F., Clissold, L., Simmonds, J.,
875 Ramirez-Gonzalez, R.H., Wang, X., Borrill, P.*, et al.* (2017). Uncovering hidden variation in polyploid
876 wheat. Proceedings of the National Academy of Sciences *114*, E913-E921.
877 Kumar, A., Pathak, R.K., Gupta, S.M., Gaur, V.S., and Pandey, D. (2015). Systems Biology for Smart
878 Crops and Agricultural Innovation: Filling the Gaps between Genotype and Phenotype for Complex
879 Traits Linked with Robust Agricultural Productivity and Sustainability. OMICS: A Journal of Integrative
880 Biology *19*, 581-601.
881 Lavarenne, J., Guyomarc'h, S., Sallaud, C., Gantet, P., and Lucas, M. (2018). The Spring of Systems
882 Biology-Driven Breeding. Trends in Plant Science *23*, 706-720.
883 Lee, S., Jeong, H., Lee, S., Lee, J., Kim, S.-J., Park, J.-W., Woo, H.R., Lim, P.O., An, G., Nam, H.G.*, et al.*
884 (2017). Molecular bases for differential aging programs between flag and second leaves during grain-
885 filling in rice. Scientific Reports *7*, 8792.
886 Leng, Y., Ye, G., and Zeng, D. (2017). Genetic Dissection of Leaf Senescence in Rice. International
887 Journal of Molecular Sciences *18*, 2686.

Leyva-González, M.A., Ibarra-Laclette, E., Cruz-Ramírez, A., and Herrera-Estrella, L. (2012). Functional and Transcriptome Analysis Reveals an Acclimatization Strategy for Abiotic Stress Tolerance Mediated by Arabidopsis NF-YA Family Members. PLOS ONE *7*, e48138.

Li, C., and Dubcovsky, J. (2008). Wheat FT protein regulates *VRN1* transcription through interactions with FDL2. The Plant Journal *55*, 543-554.

Li, G., Yu, Y., Ouyang, Y., and Yao, W. (2017). funRiceGenes dataset for comprehensive understanding and application of rice functional genes. GigaScience *7*, gix119.

Liang, C., Wang, Y., Zhu, Y., Tang, J., Hu, B., Liu, L., Ou, S., Wu, H., Sun, X., Chu, J.*, et al.* (2014). OsNAP connects abscisic acid and leaf senescence by fine-tuning abscisic acid biosynthesis and directly targeting senescence-associated genes in rice. Proceedings of the National Academy of Sciences *111*, 10013-10018.

Lin, M., Pang, C., Fan, S., Song, M., Wei, H., and Yu, S. (2015). Global analysis of the *Gossypium hirsutum* L. Transcriptome during leaf senescence by RNA-Seq. BMC Plant Biol *15*, 43.

Marchler-Bauer, A., Bo, Y., Han, L., He, J., Lanczycki, C.J., Lu, S., Chitsaz, F., Derbyshire, M.K., Geer, R.C., Gonzales, N.R.*, et al.* (2017). CDD/SPARCLE: functional classification of proteins via subfamily domain architectures. Nucleic Acids Res *45*, D200-D203.

Merchant, N., Lyons, E., Goff, S., Vaughn, M., Ware, D., Micklos, D., and Antin, P. (2016). The iPlant Collaborative: Cyberinfrastructure for Enabling Data to Discovery for the Life Sciences. PLOS Biology *14*, e1002342.

Ng, P.C., and Henikoff, S. (2003). SIFT: Predicting amino acid changes that affect protein function. Nucleic acids research *31*, 3812-3814.

Park, S.Y., Yu, J.W., Park, J.S., Li, J., Yoo, S.C., Lee, N.Y., Lee, S.K., Jeong, S.W., Seo, H.S., Koh, H.J.*, et al.* (2007). The senescence-induced staygreen protein regulates chlorophyll degradation. Plant Cell *19*, 1649-1664.

Pearce, S., Tabbita, F., Cantu, D., Buffalo, V., Avni, R., Vazquez-Gross, H., Zhao, R., Conley, C.J., Distelfeld, A., and Dubcovksy, J. (2014). Regulation of Zn and Fe transporters by the *GPC1* gene during early wheat monocarpic senescence. BMC Plant Biology *14*, 368.

Penfold, C.A., and Wild, D.L. (2011). How to infer gene networks from expression profiles, revisited. Interface focus *1*, 857-870.

Podzimska-Sroka, D., Shea, C., Gregersen, P., and Skriver, K. (2015). NAC Transcription Factors in Senescence: From Molecular Structure to Function in Crops. Plants *4*, 412.

Ramirez-Gonzalez, R.H., Borrill, P., Lang, D., Harrington, S.A., Brinton, J., Venturini, L., Davey, M., Jacobs, J., van Ex, F., Pasha, A.*, et al.* (2018). The transcriptional landscape of polyploid wheat. Science *361*.

Ramirez-Gonzalez, R.H., Segovia, V., Bird, N., Fenwick, P., Holdgate, S., Berry, S., Jack, P., Caccamo, M., and Uauy, C. (2015). RNA-Seq bulked segregant analysis enables the identification of high-resolution genetic markers for breeding in hexaploid wheat. Plant Biotechnology Journal *13*, 613-624.

Sakai, H., Lee, S.S., Tanaka, T., Numa, H., Kim, J., Kawahara, Y., Wakimoto, H., Yang, C.-c., Iwamoto, M., Abe, T.*, et al.* (2013). Rice Annotation Project Database (RAP-DB): An Integrative and Interactive Database for Rice Genomics. Plant and Cell Physiology *54*, e6.

Sakuraba, Y., Piao, W., Lim, J.H., Han, S.H., Kim, Y.S., An, G., and Paek, N.C. (2015). Rice *ONAC106* Inhibits Leaf Senescence and Increases Salt Tolerance and Tiller Angle. Plant & cell physiology *56*, 2325-2339.

Shannon, P., Markiel, A., Ozier, O., Baliga, N.S., Wang, J.T., Ramage, D., Amin, N., Schwikowski, B., and Ideker, T. (2003). Cytoscape: a software environment for integrated models of biomolecular interaction networks. Genome research *13*, 2498-2504.

Soneson, C., Love, M., and Robinson, M. (2016). Differential analyses for RNA-seq: transcript-level estimates improve gene-level inferences [version 2; referees: 2 approved]. F1000Research *4*.

Thomas, H., and Howarth, C.J. (2000). Five ways to stay green. Journal of Experimental Botany *51*, 329-337.

938 Uauy, C., Distelfeld, A., Fahima, T., Blechl, A., and Dubcovsky, J. (2006). A NAC Gene Regulating
939 Senescence Improves Grain Protein, Zinc, and Iron Content in Wheat. Science *314*, 1298-1301.
940 Uauy, C., Paraiso, F., Colasuonno, P., Tran, R.K., Tsai, H., Berardi, S., Comai, L., and Dubcovsky, J. (2009).
941 A modified TILLING approach to detect induced mutations in tetraploid and hexaploid wheat. BMC
942 Plant Biology *9*, 115.
943 Wickham, H. (2016). ggplot2: Elegant Graphics for Data Analysis (Springer-Verlag New York).
944 Wolfe, K.H., Gouy, M., Yang, Y.W., Sharp, P.M., and Li, W.H. (1989). Date of the monocot-dicot
945 divergence estimated from chloroplast DNA sequence data. Proceedings of the National Academy of
946 Sciences *86*, 6201-6205.
947 Woo, H.R., Kim, H.J., Nam, H.G., and Lim, P.O. (2013). Plant leaf senescence and death – regulation by
948 multiple layers of control and implications for aging in general. Journal of Cell Science *126*, 4823-4833.
949 Woo, H.R., Koo, H.J., Kim, J., Jeong, H., Yang, J.O., Lee, I.H., Jun, J.H., Choi, S.H., Park, S.J., Kang, B.*, et*
950 *al.* (2016). Programming of Plant Leaf Senescence with Temporal and Inter-Organellar Coordination of
951 Transcriptome in Arabidopsis. Plant Physiology *171*, 452-467.
952 Wu, A., Allu, A.D., Garapati, P., Siddiqui, H., Dortay, H., Zanor, M.I., Asensi-Fabado, M.A., Munne-
953 Bosch, S., Antonio, C., Tohge, T.*, et al.* (2012). *JUNGBRUNNEN1*, a reactive oxygen species-responsive
954 NAC transcription factor, regulates longevity in Arabidopsis. Plant Cell *24*, 482-506.
955 Wu, L., Ren, D., Hu, S., Li, G., Dong, G., Jiang, L., Hu, X., Ye, W., Cui, Y., Zhu, L.*, et al.* (2016). Down-
956 Regulation of a Nicotinate Phosphoribosyltransferase Gene, *OsNaPRT1*, Leads to Withered Leaf Tips.
957 Plant Physiology *171*, 1085-1098.
958 Yan, L., Loukoianov, A., Tranquilli, G., Helguera, M., Fahima, T., and Dubcovsky, J. (2003). Positional
959 cloning of the wheat vernalization gene *VRN1*. Proceedings of the National Academy of Sciences *100*,
960 6263-6268.
961 Zadoks, J.C., Chang, T.T., and Konzak, C.F. (1974). A decimal code for the growth stages of cereals.
962 Weed Research *14*, 415-421.
963 Zhang, Q., Xia, C., Zhang, L., Dong, C., Liu, X., and Kong, X. (2018). Transcriptome Analysis of a
964 Premature Leaf Senescence Mutant of Common Wheat (*Triticum aestivum* L.). International Journal
965 of Molecular Sciences *19*, 782.
966 Zhang, W.Y., Xu, Y.C., Li, W.L., Yang, L., Yue, X., Zhang, X.S., and Zhao, X.Y. (2014). Transcriptional
967 Analyses of Natural Leaf Senescence in Maize. PLOS ONE *9*, e115617.
968 Zhao, D., Derkx, A.P., Liu, D.-C., Buchner, P., and Hawkesford, M.J. (2015). Overexpression of a NAC
969 transcription factor delays leaf senescence and increases grain nitrogen concentration in wheat. Plant
970 Biology *17*, 904-913.

971

972